SCIENCE CHINA
Information Sciences

• RESEARCH PAPER •

June 2017, Vol. 60 062401:1–062401:12
doi: 10.1007/s11432-016-0037-0

High-speed visual target tracking with mixed rotation invariant description and skipping searching

Yongxing YANG[1], Jie YANG[2], Zhongxing ZHANG[1], Liyuan LIU[1] & Nanjian WU[1]*

[1]*State Key Laboratory for Superlattices and Microstructures, Institute of Semiconductors, Chinese Academy of Sciences, Beijing* 100083*, China;*
[2]*Department of Electrical and Computer Engineering, University of Calgary, Calgary* T2N1N4*, Canada*

Received April 6, 2016; accepted May 7, 2016; published online December 8, 2016

Abstract This paper proposes a novel high-speed visual target tracking system based on mixed rotation invariant description (MRID) and skipping searching method. MRID is a novel rotation invariant description of texture and edge information by annular histograms and dominant direction. It overcomes rotation variant and large computation issues in conventional LBP-HOG feature description. The skipping searching method used in tracking can remarkably decrease the computation time by avoiding repeated searching operations. The proposed tracking system contains an image sensor, a hierarchical vision processor and an actuator with 2 dimensions of freedom (DOF). The vision processor integrates processors with pixel- and row-level parallelism to speed up the tracking algorithm. Experiment results show that the proposed system can achieve over 1000-fps processing speed of the tracking algorithm under 750 × 480 resolution image.

Keywords target tracking, parallel vision processor, MRID, skipping searching, image processing

Citation Yang Y X, Yang J, Zhang Z X, et al. High-speed visual target tracking with mixed rotation invariant description and skipping searching. Sci China Inf Sci, 2017, 60(6): 062401, doi: 10.1007/s11432-016-0037-0

1 Introduction

Target tracking is one of the most fundamental technologies in computer vision. Many tracking systems have been designed for various applications such as industrial automation, autonomous robot navigation, intelligent video surveillance, activity analysis, classification and recognition from motion, and human-computer interfaces [1, 2]. However, the respond speed of conventional tracking system is limited to less than 60 fps due to serial image processing. Some researchers adopt parallel single-instruction-multiple-data (SIMD) processors to speed up tracking algorithms [3–7]. However, these processors are still unable to meet the needs of high-speed target tracking applications because they can only implement straightforward low-level and some simple middle-level image processing algorithms such as background subtraction, segmentation and motion detection.

In many applications such as robot navigation and automatic drive, the target moves at high speed in complex environment. In order to tracking a moving target constantly, not only real-time processing capacity but also robust algorithms are required. Image processing algorithms such as optical flow,

* Corresponding author (email: nanjian@red.semi.ac.cn)

self-window and moment tracking have been implemented on high-speed vision systems to realize fast tracking functions [8–10]. However, most of them can only be applied to certain scenarios with a clear background or constant illumination. Some other algorithms such as compressive tracking and tracking-learning-detection have better performance in robustness; however, their computation overhead constrains their real-time performance [11, 12]. Local binary pattern (LBP)-histogram of gradient (HOG) feature description is widely used in target detection and tracking [13, 14]. However, both of the HOG and LBP histogram are rotation variant. Hence, it would result in target shifting and tracking failing when the target moves in a complicated environment or rotates suddenly.

In this paper, we propose a mixed rotation invariant description (MRID) and skipping searching based tracking algorithm and a novel high-speed visual target tracking system. This MRID is invariant to rotation and illumination changes so that it achieves more robust tracking than previously reported fast tracking algorithms. The skipping searching method can remarkably decrease the computation time, because it avoids the repeated searching operations during tracking. The proposed tracking system contains an image sensor, a hierarchical vision processor and an actuator. The vision processor integrates processors with pixel- and row-level parallelism to speed up the tracking algorithm. The system with hierarchical parallelism can achieve a system performance of over 1000-fps processing speed in complex scenes.

The rest of the paper is organized as follows. Section 2 describes the MRID and the corresponding tracking algorithm. In section 3, the proposed vision processor is introduced. Section 4 presents the implementation of our tracking system. Section 5 illustrates the experiment results and correlative analysis. Finally section 6 concludes this paper.

2 High-speed MRID tracking with skipping searching

This paper proposes a novel MRID feature description and the corresponding tracking algorithm with skipping searching. These increase the robustness of the tracking system and decrease the computation time to achieve reliable high-speed target tracking. The MRID description and the tracking algorithm are presented in the following parts.

2.1 MRID description

LBP-HOG is a very efficient local feature description. It has been used in various applications such as pedestrian detection and tracking. However, both of the HOG and LBP histogram are rotation variant. When the target suffers from complicated motion and sudden rotation, LBP-HOG description will degenerate and even cease to be effective. The proposed MRID description adopts mixed annular LBP histogram and annular gradient histogram with a dominant direction to describe the texture and edge information of target, as shown in Figure 1. It is a novel rotation invariant description.

In annular gradient histogram (process A), first (step 1) the horizontal (∇x) and vertical (∇y) gradients of each pixel are calculated by masks [–1 0 1] and $[-1\ 0\ 1]^{\mathrm{T}}$, respectively. The magnitude (r) and orientation (ϕ) of gradient are calculated as (1).

$$r = \sqrt{(\nabla x)^2 + (\nabla y)^2}, \quad \phi = \arctan \frac{\nabla y}{\nabla x}. \tag{1}$$

However, this conventional gradient calculation limits processing speed greatly because it involves some costly operations such as square, division, and arctangent. To speed up the calculation, the magnitude

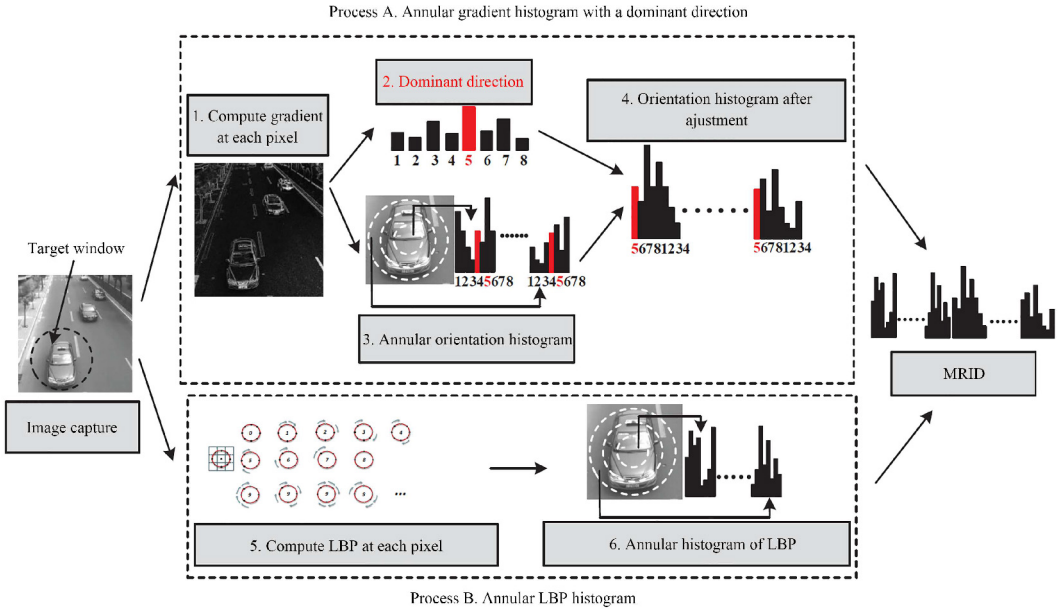

Figure 1 (Color online) Process of the proposed MRID.

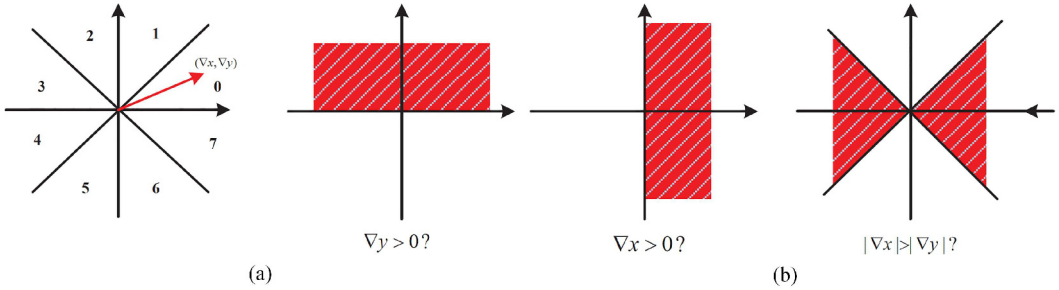

Figure 2 (Color online) Gradient orientation with boundary comparison. (a) Orientation assignment; (b) three boundary conditions for orientation assignment.

(r) and orientation (ϕ) are simplified as (2).

$$r' = |\nabla x| + |\nabla y|,$$
$$\phi' = \begin{cases} 0, & \nabla x > 0, \nabla y \geqslant 0, |\nabla x| > |\nabla y|; \\ 1, & \nabla x > 0, \nabla y > 0, |\nabla x| \leqslant |\nabla y|; \\ 2, & \nabla x \leqslant 0, \nabla y > 0, |\nabla x| < |\nabla y|; \\ 3, & \nabla x < 0, \nabla y > 0, |\nabla x| \geqslant |\nabla y|; \\ 4, & \nabla x < 0, \nabla y \leqslant 0, |\nabla x| > |\nabla y|; \\ 5, & \nabla x < 0, \nabla y < 0, |\nabla x| \leqslant |\nabla y|; \\ 6, & \nabla x \geqslant 0, \nabla y < 0, |\nabla x| < |\nabla y|; \\ 7, & \nabla x > 0, \nabla y < 0, |\nabla x| \geqslant |\nabla y|. \end{cases} \tag{2}$$

The magnitude is calculated by the sum of the absolute value. The orientation is divided into 8 bins with the range of 45°. Three boundary conditions are used to decide which bin the orientation belongs to, as shown in Figure 2.

In step 2, the histogram of orientation ϕ' in the target window is obtained and the highest peak is detected as the dominant direction of the target. Compared with conventional cellular histogram, the target window is a circular patch instead of rectangle region. In step 3, the circular target region is subdivided into annular spatial bins (shown in Figure 3) to improve distinctiveness while maintaining

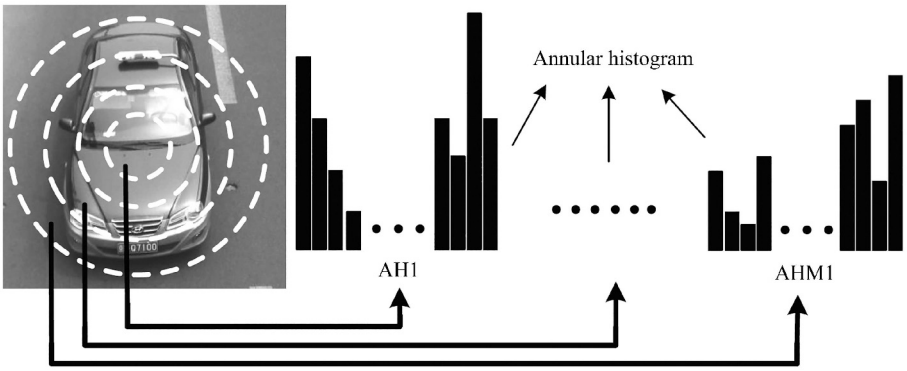

Figure 3 Extraction of annular histogram.

rotation invariance. Assuming that the diameter of object region is N_1 pixels, the region is divided into M_1 annulus. The orientation histograms of these M_1 annulus are concatenated and the order of bins is adjusted according to the dominant direction in step 4.

In annular LBP histogram (process B), at first (step 5) the uniform LBP of each pixel is calculated as (3) descripted in [15].

$$\mathrm{LBP}_{\mathrm{P,R}} = \begin{cases} \sum_{i=0}^{p-1} s(g_i - g_c), & U \leqslant 2; \\ p+1, & U > 2, \end{cases} \tag{3}$$

where

$$U = |s(g_{p-1} - g_c) - s(g_0 - g_c)| + \sum_{i=1}^{p-1} |s(g_i - g_c) - s(g_{i-1} - g_c)|,$$

$$s(x) = \begin{cases} 1, x \geqslant 0; \\ 0, x < 0, \end{cases}$$

g_c corresponds to the grayscale value of the central pixel and $g_i (i = 0, ..., p-1)$corresponds to the grayscale values of p pixels equally lied on a circle of radius R that form a circularly symmetric neighbor set.

Then the LBP histogram of the annular object window is obtained in step 6. At last, the annular LBP histogram and annular gradient histogram with a dominant direction are concatenated to form a rotation invariant feature of the object. Compared with conventional LBP-HOG feature, MRID overcomes rotation variant and large computation issues.

2.2 Tracking algorithm

Figure 4 shows the flow chart of the tracking algorithm based on the MRID feature and skipping searching. It mainly contains operations such as noise suppression, MRID feature extraction, skipping searching, Adaboost classification and target capture. The details are explained below.

Skipping searching: In high speed tracking system, the difference between two successive frames will be limited to several pixels, and the speed of the target will not change abruptly. Hence, the search windows are surrounding the location of target center, as shown in Figure 4. In conventional tracking algorithms shown in Figure 5 (a), the position $(Sx_{i,j},\ Sy_{k,j})$ of center of search window in j-th frame can be presented as (4).

$$\begin{aligned} Sx_{i,j} &= x_{j-1} - dx + i, \quad i \in [0, 2 \times dx], \\ Sy_{k,j} &= y_{j-1} - dy + k, \quad k \in [0, 2 \times dy], \end{aligned} \tag{4}$$

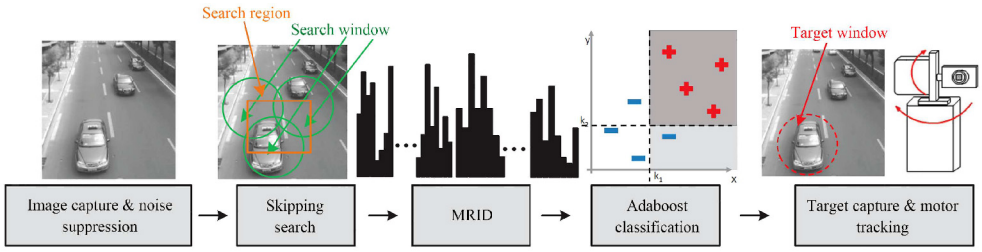

Figure 4 (Color online) Process of MRID-based tracking algorithm with skipping search.

where (x_{j-1}, y_{j-1}) is the position of the target center in j-1st frame (red star in Figure 5(a)), the max displacement of the target between two successive frames are dx and dy pixels in horizontal and vertical directions, respectively.

The searching region (the region which contains centers of all the search windows) in j-th frame is shown as the yellow region in Figure 5(a). It insures to capture the target by searching every possible position and costs $(2 \times dx + 1) \times (2 \times dy + 1)$ searching time. However, it brings in great computation redundancy and limits tracking speed.

In our skipping searching method shown in Figure 5 (b), searching computation time is greatly compressed by considering motion information. Different searching granularity is adopted for different positions: positions with larger possibility (near the predicted position) to be the target are assigned with fine granularity; positions with less possibility (far from the predicted position) are with coarse granularity. The position of center of search window $(Sx_{i,j},\ Sy_{k,j})$ in j-th frame is presented in (5),

$$\begin{aligned} Sx_{i,j} &= \begin{cases} x_{j-1} + dx_{j-1} - \frac{dx}{sk1} + i, & i \in [0, \frac{2\times dx}{sk1}); \\ x_{j-1} - dx + \alpha \times i + \beta \times 2dx, & i \in [\frac{2\times dx}{sk1}, \frac{2\times dx}{sk2}], \end{cases} \\ Sy_{k,j} &= \begin{cases} y_{j-1} + dy_{j-1} - \frac{dy}{sk1} + k, & k \in [0, \frac{2\times dy}{sk1}); \\ y_{j-1} - dy + \alpha \times k + \beta \times 2dy, & k \in [\frac{2\times dy}{sk1}, \frac{2\times dy}{sk2}], \end{cases} \end{aligned} \tag{5}$$

where $\alpha = \frac{sk1\times sk2}{sk1-sk2}$, $\beta = -\frac{sk2}{sk1-sk2}$, $sk1$ and $sk2$ are two skipping factors, $sk1 > sk2 > 1$,

$$dx_{j-1} = \begin{cases} x_{j-1} - x_{j-2}, & j \geqslant 2; \\ 0, & \text{else}; \end{cases}$$

$$dy_{j-1} = \begin{cases} y_{j-1} - y_{j-2}, & j \geqslant 2; \\ 0, & \text{else}, \end{cases}$$

$sk1$ controls the searching region of fine granularity; $sk2$ represents the compressing factor of the whole skipping searching. The bigger $sk1$ and $sk2$ are, the coarser the searching granularity is.

Compared to conventional searching method, the search region in our method (shown in Figure 5(b)) is much sparser; it decreases the computation time by an order of $O(sk2^2)$ with little loss of searching accuracy.

MRID feature extraction: The MRID of search window is extracted to form a global feature of the target. This feature vector represents edges, texture and spatial information of the target.

Adaboost classification: The MRID is classified by the adaboost classifier [16]. It combines K weak classifiers $l(i)$ with a specific weight $\alpha(i)$ to form a strong classifier as shown in (6).

$$C = \sum_{i=0}^{K-1} \alpha(i) \times l(\,\mathrm{MRID}(i) - T(i)\,), \tag{6}$$

where $l(\mathrm{MRID}(i) - T(i)\,) = \begin{cases} 1, & \mathrm{MRID}(i) - T(i) \geqslant 0; \\ -1, & \text{otherwise}. \end{cases}$

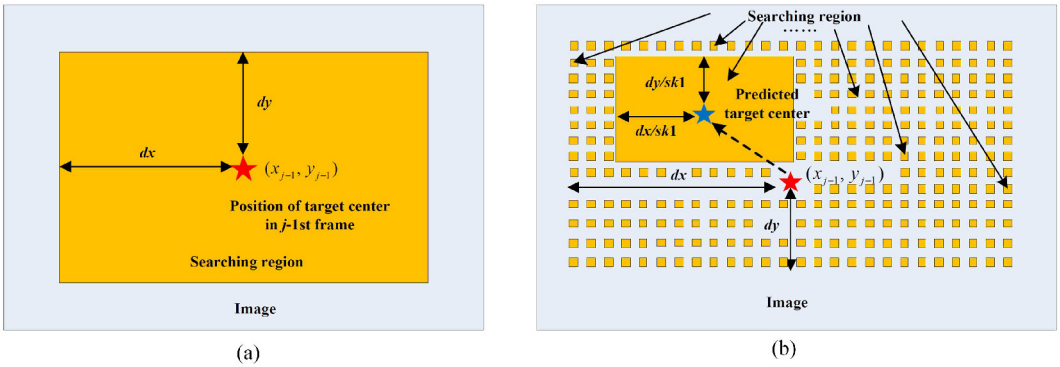

Figure 5 Searching region in conventional tracking (a) and skipping searching method (b), the red star presents the position of target center in j-1st frame, the blue star presents the position of predicted target center in j-th frame.

The weak classifier $l(i)$ consists of a feature MRID(i) which corresponds to a single MRID histogram bin and a threshold vector $T(i)$ corresponding to MRID(i). Both $\alpha(i)$ and $T(i)$ are obtained with adaboost training algorithm [16]. The value C of search window shows the classification result: target or not. If C is larger, the search window is more likely to be the target.

Target capture and motor tracking: Then the search window with the largest C is updated as the target window during tracking. Then directions and angles for motor rotation are calculated according to the position of the target. Then the processor sends control pulse to motors and makes the camera gaze at the target.

3 Hierarchical parallel vision processor

In this section, the proposed processor is introduced. It is motivated by the modern visual target tracking pipeline. In this pipeline, the image sensor captures the image of the targets at high speed. The processor suppresses the image noise first, then searches the target by the skipping searching method and extracts its feature, and finally controls the actuator to track the target.

The proposed vision processor is shown in Figure 6. It contains an $M \times M$ processing element (PE) array, an $M \times 1$ row processor (RP) array, a dual-core MPU (Microprocessor Unit) and a motor controller. The pixel-parallel PE array and row-parallel RP array can speed up low-level and middle-level image processing operations by $O(M^2)$ and $O(M)$, respectively. Each PE consists of a piece of local memory, a temporary register, several multiplexers and a 1-bit ALU performing operations such as and, or, addition, and inversion. RP consists of a local memory, a register file, some multiplexers, and an 8-bit ALU. The ALU can carry out operations such as max/min selection, absolute value calculation, subtraction and addition.

Compared with previous SIMD processors [17–21], this processor improves its flexibility with little circuit cost. For some operations such as annular histogram calculation, SIMD manner will result in inefficiency and even errors (For example, a rectangle histogram instead of an annular histogram is calculated because all the PE/RP work simultaneously). Multiple-instruction-multiple-data (MIMD) is a solution but it costs a lot. In the proposed processor, there is an "active flag" (rectangle in Figure 6) in each PE and RP. The PE/RP works only when the active flag equals to 1 (presented as the red PE and RP in Figure 6). This flag can be set by instructions in prior or calculated during tracking. This design only costs several additional logic gates compared with SIMD processors but it achieves better flexibility than the original processor.

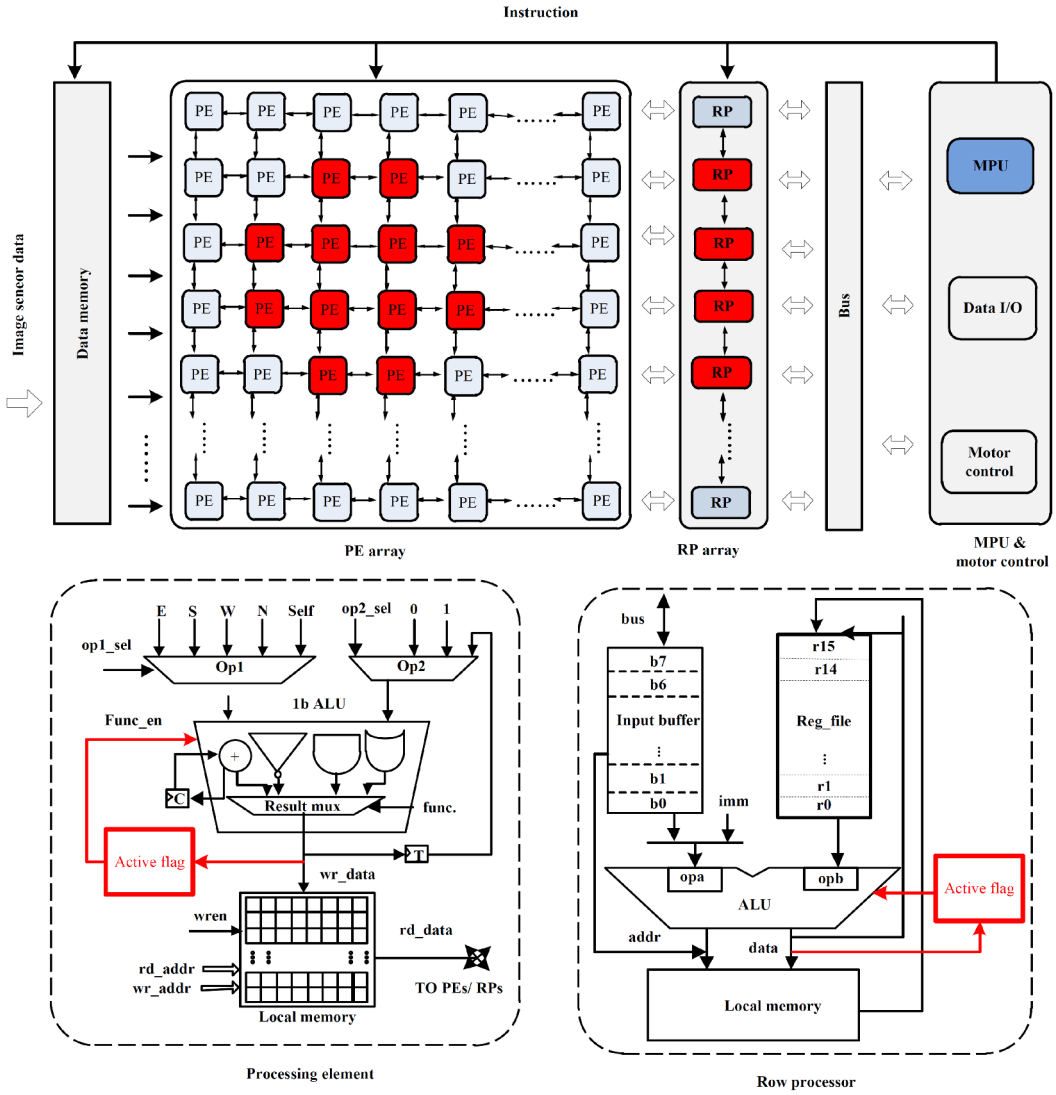

Figure 6 (Color online) Proposed vision processor.

4 System implementation

The tracking algorithm is implemented on a high-speed target tracking system, as shown in Figure 7. The used CMOS image sensor is a global shutter image sensor with a resolution of 750 × 480. In target tracking applications, valuable target region is about hundreds to thousands pixels and most of the other pixels are useless background. So only the 256 × 256 pixels region-of-interest (ROI) is transmitted to the processor to reduce bandwidth overhead. The vision processor and other necessary blocks were implemented on an ArriaV FPGA device. The information about consumed FPGA hardware resource is listed in Table 1. In this prototype, it consists of a 128 × 128 PE array, a 128 RP array and an MPU; the operating frequency is 100 MHz. The FPGA device is linked to a personal computer (PC) through the Ethernet interface. Instructions for hierarchical parallel processor were first developed and compiled on PC, and then sent to memories on FPGA device. The PC was also responsible for video monitor during test.

The main parameters of tracking algorithm are shown in Table 2. The choice of parameter affects both the tracking accuracy and computational complexity. It is a trade-off. Based on our experiment in both video sequences and real sceneries, this parameter configuration can result in satisfying tracking. The noise suppression, gradient and LBP calculation operations can be carried out by PE. RP can extract

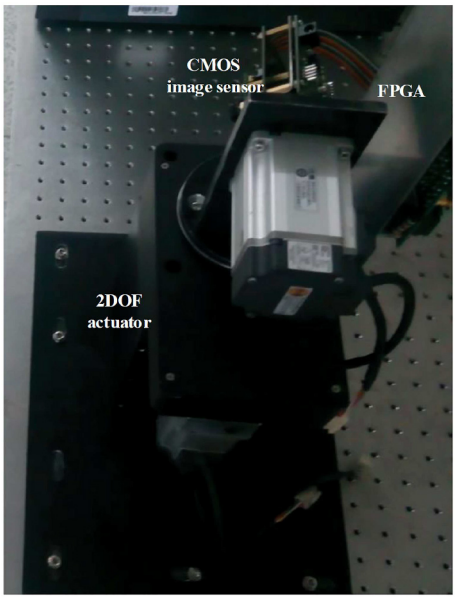

Figure 7 (Color online) Photograph of tracking system.

Table 1 FPGA resource ultilization

FPGA device	ArriaV 5AGXFB3H4F35C4N
Logic utilization (in ALMs)	83845/136880 (61%)
Total registers	83534
Total pins	41/656 (6%)
Total block memory bits	2350280/17674240 (13%)
Total PLLs	2/36 (6%)

Table 2 Parameters of algorithm

Parameter	Value	Description
N_1	96	Diameter of object region
M_1	3	Number of annulus
P	8	Parameter of LBP
R	1	Parameter of LBP
$sk1$	3	Skipping factor
$sk2$	2	Skipping factor
dx	7	Max speed of the target
dy	7	Max speed of the target

histogram and calculate the classifier C. The MPU captures the target position and controls the motors tracking.

Table 3 shows the execution time of some kernel functions of the algorithm. The LBP was calculated within 400 instruction cycles. The classification calculation cost 134 instruction cycles. It takes 300 instruction cycles to control the actuator. The breakdown of time for the proposed vision processor performing the tracking algorithm is 792 μs (1260 fps).

5 Experiment results

This section presents the system performances of the target tracking system mentioned in the previous section.

Firstly, experiments were carried out to evaluate the basic performance of the tracking algorithm. The MRID histograms of a jeep model with different angles are obtained. Thanks to the rotation invariant

Table 3 Execution time of algorithm

Function	Instruction cycle	Time(ms)
$LBP_{8,1}$	353	3.5
Gradient	122	1.2
Annular histogram of LBP	800	8.0
Annular orientation histogram	640	6.4
Dominant direction	20	0.2
Adaboost classification	134	1.3
Motor control	300	3.0

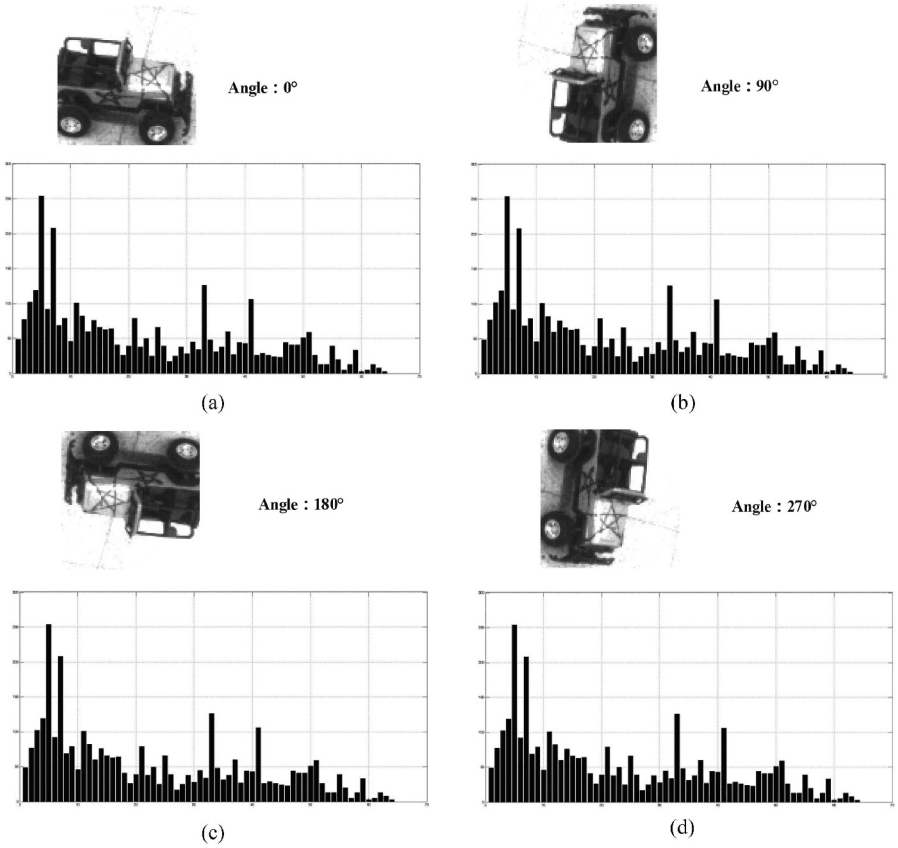

Figure 8 MRID of a jeep model with different angles. (a) Angle 0; (b) angle 90; (c) angle 180; (d) angle 270.

feature, these vectors are the same, as shown in Figure 8.

Then we evaluate our tracking algorithm on some challenging sequences which are publicly available. Some screenshots of the tracking result are shown in Figure 9. The red circles present the targets position. It can be seen that our tracking algorithm achieves satisfying performance in most sequences, even with complicated motion and large degrees of rotation. Furthermore, our tracker runs fast with the help of our vision processor.

Next, we made some experiments of mechanical tracking of a moving car and human hand obtained by controlling the 2 DOF actuator. Constrained by the limited experimental space, it is difficult to track real vehicle with our system. So we used models to estimate our tracking systems. Figure 10 shows the environment setup for the experiment.

Figures 11 and 12 show the result of the target tracking. The actuator tracks the target at the center of view, as shown in the photos. Figures 11(d) and 12(d) show the x and y coordinate valves of its center positions during tracking. It can be seen that the center position of the target image was always controlled around the center of the camera view. The small deviations were mainly caused by the

Figure 9 Screenshots of tracking result. Highlighting instances of (a) and (c) scale and illumanation change; (b) out of plane rotation; (d) heavy occlusion; (e) and (f) abrupt motion.

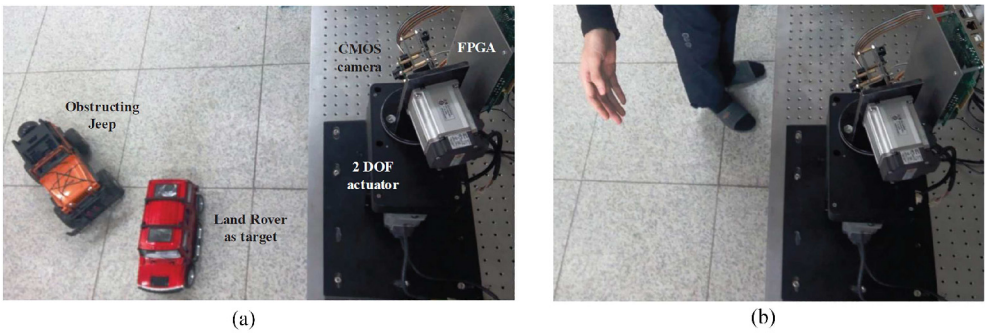

Figure 10 Environment setup for the experiment. (a) Car tracking; (b) hand tracking.

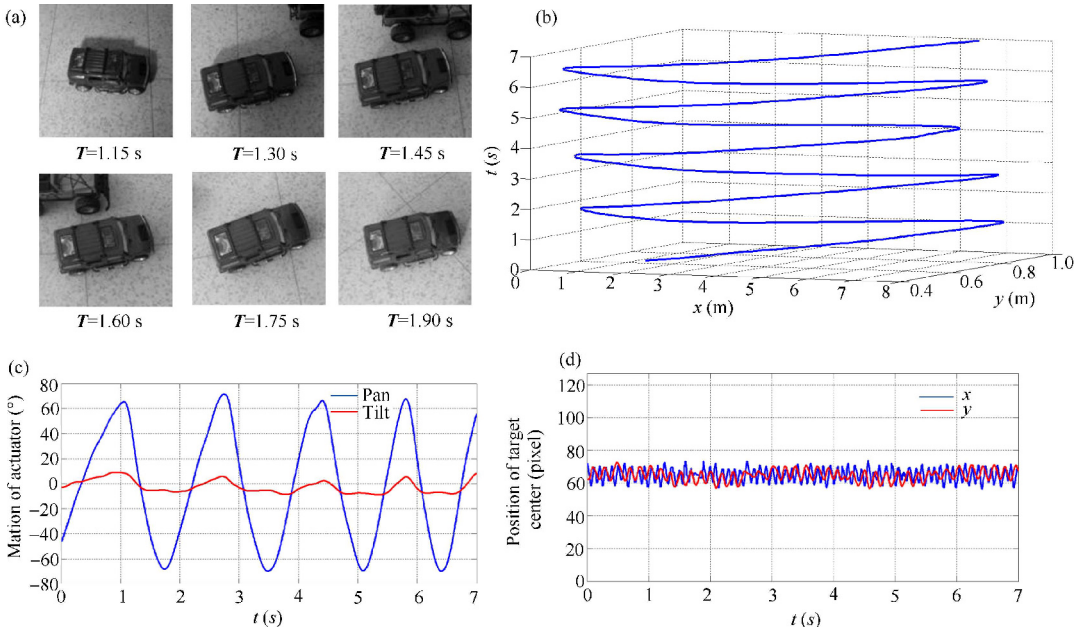

Figure 11 Results of car tracking. (a) Photos captured during tracking; (b) trajectory of car; (c) trajectory of the tilt motor (red line) and the pan motor (blue line); (d) x (blue line) and y (red line) coordinate of target center.

limitation of motor potential ability. The trajectories of the actuator are also given in Figures 11(c) and 12(c). The tilt (red line) and pan (blue line) movement correspond to the periodical motion of the target.

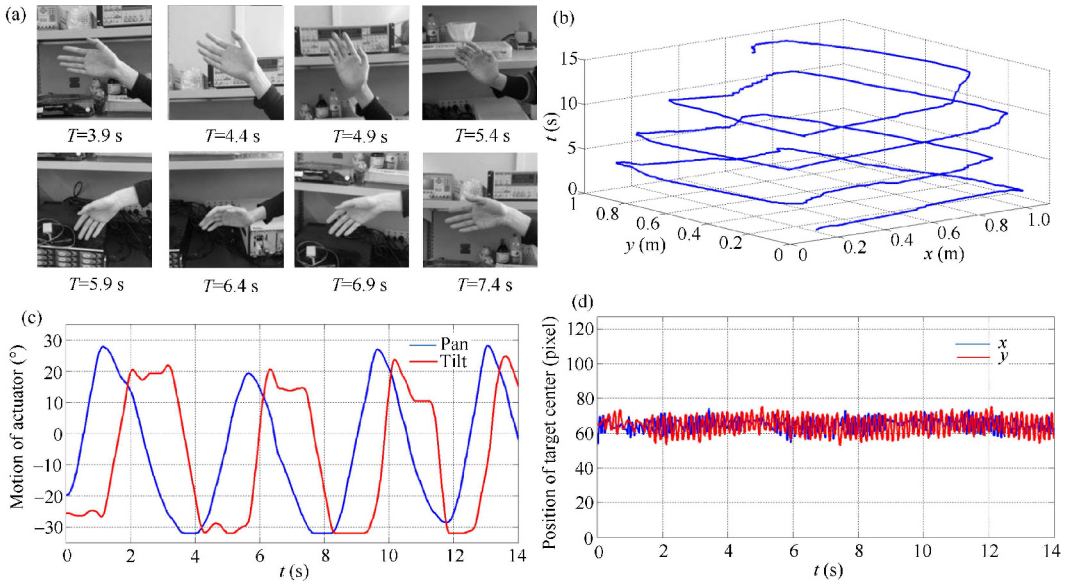

Figure 12 Results of hand tracking. (a) Photos captured during tracking; (b) trajectory of human hand; (c) trajectory of the tilt motor (red line) and the pan motor (blue line); (d) x (blue line) and y (red line) coordinate of target center.

Table 4 Comparison with related work

	This work	Ref. [20]	Ref. [2]	Refs. [13, 14]
Image	8-bit mono	8-bit mono	8-bit color	8-bit mono
Algorithm	MRID based	LBP based	Color tracking	HOG-LBP
Resolution	750 × 480	128×128	512×512	N/A
Environment setting	Outdoor/indoor, Complex sceneries, Changing illumination, Abrupt rotation	Indoor, Certain sceneries, Changing illumination	Indoor, Certain sceneries, Changing illumination	Outdoor/indoor, Certain sceneries, Changing illumination
Robustness	Best	Common	Worst	Common
Tracking Method	Learning	No learning	No learning	Learning
Frequency (MHz)	100	50	151.2	N/A
Processing speed (fps)	1200	1000	2000	N/A

The experiment results indicate that the system can achieve successful tracking even if the target moves fast and irregularly.

Table 4 shows a comparison with previously reported tracking systems. In [21] color images are used to achieve an extremely fast tracking, they adopt several thresholds to convert a HSV (Hue Saturation Value) image to a binary image. This method will lose the target when the color of background and target are similar. In [13, 14, 21], a LBP and LBP-HOG based tracking algorithm is implemented. They are more robust in environments with complex background and changing illumination. However, both of them use cellular histogram and neither is rotation invariant. This will result in failure when tracking objects with sudden rotation. Our proposed tracking algorithm adopts a robust MRID feature which can work in a more complex environment with large degrees of rotation and abrupt motion. Furthermore, the hierarchical processor is more flexible than original SIMD processor and it greatly enhances the speed of our tracking algorithm to over 1000-fps.

6 Conclusion

In this paper, a high-speed tracking system with MRID target tracking algorithm was proposed. It consists of an image sensor, a parallel vision processor and an actuator to realize high-speed tracking. The vision

processor integrates hierarchical processors to speed up operations from local descriptor calculation to target capture during tracking. The tracking algorithm with MRID and skipping searching was proposed. Compared with conventional LBP-HOG feature, MRID overcomes rotation variant and large computation issues. Skipping searching remarkably decrease the computation by avoiding the repeated searching operations. This tracking algorithm can be carried out on the system within 1ms. The efficacy of our proposed system was verified in the real-time experiment for tracking a fast moving target under complex conditions.

Acknowledgements This work was supported by the National Natural Science Foundation of China (Grant Nos. 61234003, 61434004, 61504141) and CAS Interdisciplinary Project (Grant No. KJZD-EW-L11-04).

Conflict of interest The authors declare that they have no conflict of interest.

References

1 Yilmaz A, Javed O, Shah M, et al. Object tracking: a survey. Acm Comput Surv, 2006, 38: 81–93
2 Wu Y, Lim J, Yang M, et al. Object tracking benchmark. IEEE Trans Pattern Anal, 2015, 37: 1834–1848
3 Ishikawa M, Ogawa K, Komuro T, et al. A CMOS vision chip with SIMD processing element array for 1 ms image processing. In: Proceedings of IEEE International Solid-State Circuits Conference, San Francisco, 1999. 206–207
4 Komuro T, Ishii I, Ishikawa M, et al. A digital vision chip specialized for high-speed target tracking. IEEE Trans Elec Dev, 2003, 50: 191–199
5 Komuro T, Kagami S, Ishikawa M, et al. A dynamically reconfigurable SIMD processor for a vision chip. IEEE J Sol St Circ, 2004, 39: 265–268
6 Yamada Y, Ishikawa M. High speed target tracking using massively parallel processing vision. In: Proceedings of IEEE/RSJ International Conference on Intelligent Robots and Systems, Tokyo, 1993. 267–272
7 Miao W, Lin Q, Zhang W, et al. A programmable SIMD vision chip for real-time vision applications. IEEE J Sol St Circ, 2008, 43: 1470–1479
8 Namiki A, Imai Y, Ishikawa M, et al. Development of a high-speed multifingered hand system and its application to catching. In: Proceedings of IEEE/RSJ International Conference on Intelligent Robots and Systems, Las Vegas, 2003. 3: 2666–2671
9 Nakamura Y, Kishi K, Kawakami H, et al. Heartbeat synchronization for robotic cardiac surgery. In: Proceedings of the International Conference on Robotics and Automation, Seoul, 2001. 2: 2014–2019
10 Nie Y, Ishii I, Yamamoto K, et al. Real-time scratching behavior quantification system for laboratory mice using high-speed vision. J Real-Time Imag Proc, 2009, 4: 181–190
11 Wu J, Chen D, Yi R. Real-time compressive tracking with motion estimation. In: Proceedings of IEEE International Conference on Robotics and Biomimetics, Shenzhen, 2013. 2374–2379
12 Zdenek K, Krystian M, Jiri M, et al. Tracking-learning-detection. IEEE Trans Pattern Anal, 2011, 34: 1409–1422
13 Li B, Yang C, Zhang Q, et al. Condensation-based multi-person detection and tracking with HOG and LBP. In: Proceedings of IEEE International Conference on Information and Automation, Hailar, 2014. 267–272
14 Qing C, Dickinson P, Lawson S, et al. Automatic nesting seabird detection based on boosted HOG-LBP descriptors. In: Proceedings of IEEE International Conference on Image Processing, Brussels, 2011. 3577–3580
15 Ojala T, Pietikainen M, Maenpaa T, et al. Multiresolution gray-scale and rotation invariant texture classification with local binary patterns. IEEE Trans Pattern Anal, 2002, 24: 971–987
16 Viola P, Jones M J. Robust Real-Time Face Detection. Int J Comput Vis, 2004, 57: 137–154
17 Shi C, Yang J, Han Y, et al. A 1000fps vision chip based on a dynamically reconfigurable hybrid architecture comprising a PE array and self-organizing map neural network. In: Proceedings of IEEE International Solid-State Circuits Conference, San Francisco, 2014. 128–129
18 Yang Y, Yang J, Liu L, et al. High-speed target tracking system based on a hierarchical parallel vision processor and gray-level LBP algorithm. IEEE Trans Syst Man Cybernet: Syst, "In press"
19 Zhang W, Fu Q, Wu N J, et al. A programmable vision chip based on multiple levels of parallel processors. IEEE J Sol St Circ, 2011, 46: 2132–2147
20 Yang J, Shi C, Liu L, et al. Heterogeneous vision chip and LBP-based algorithm for high-speed tracking. Elect Lett, 2014, 50: 438–439
21 Gu Q, Noman A A, Aoyama T, et al. A fast color tracking system with automatic exposure control. In: Proceedings of IEEE International Conference on Information and Automation, Yinchuan, 2013. 1302–1307